

Supporting Information

Nonlinear Optical Properties of Stable Cs-doped FAPbBr₃ Core@Shell Layered Perovskite Nanocrystals: Superior Temperature Sensing and Flexible Fiber-Based Pure Green LEDs

Ashutosh Mohapatra,^{1,} Smaranika Ray,¹ Prabhukrupa C Kumar,¹ Rajat Kumar Das,² Pragalbh Kashyap,³ Saikat Bhaumik^{3,*}*

1. Characterization techniques and sample preparations:

1.1. UV-VIS absorption and PL measurements: UV-1900i SHIMADZU was used to record the UV-Vis absorption spectra. Ocean Insight Maya 2000 Pro-high-sensitivity spectrometer was used to record the PL spectra using the excitation wavelength of λ_{ex} = 370 nm for all the samples. All the synthesized NCs were diluted in toluene. Further, they were transported to a quartz cuvette for the measurements.

1.2. PXRD measurement: The concentrated NCs dispersed in toluene were drop cast on the well-cleaned glass substrate 1 x 1 cm. Bruker D8 diffractometer was used to measure the P-XRD with $Cu-K_{\alpha}$ (λ = 1.54 Å) as incident radiation at 40 kV and 30 mA power. PANalytical Expert's high score plus software was used to analyze the XRD data.

1.3. TEM imaging: All the samples in toluene with an optimum solution concentration were dropped on the carbon-coated Cu grids with 200 mesh. The Jeol-TEM-2100 PLUS microscope was used to measure the TEM and operated at 200 kV.

1.4. FTIR measurement: A few microliters of concentrated solutions of NCs were drop cast to prepare the thin films. Bruker Alpha-T spectrometer was used to measure the FTIR spectra after placing the thin films on the sample holder.

1.5. FESEM and EDAX measurements: JEOL (JSM-7610F plus) instrument was used to take the FESEM image and EDS spectrum. The NCs' film was prepared by drop-casting the solution. Then, the photograph was taken at an accelerating voltage of 5 KV and a working distance of 6.8 mm.

1.6. XPS measurement: The Omicron (series 0571) electron spectrometer was used for the XPS characterization. The NCs' thin film was prepared and exposed to a beam of X-rays, which excites the atoms on the sample's surface.

1.7. Raman Spectroscopy: The Laser Micro Raman System (Model- LabRam HR, Horiba JobinYvon) was used to measure Raman. The NCs' films were prepared, and a wavelength laser (633 nm) was used to excite the NCs.

1.8. Fluorescence microscopy: Fluorescence microscopy of NCs and fibers films was performed using a Nikon Eclipse Ci (Y-TV55) fluorescence microscope.

1.9. Contact angle measurement: The contact angles of NCs and fibers films were recorded using a Kyowa DME-211 contact angle meter.

1.10. Stability tests against heat and ion migration: Stability tests for all the NCs were conducted under open-air atmospheric room conditions with 55-65% humidity. These tests evaluated the nanocrystals' resistance to ion migration and their performance under heat treatment. All the tests were performed under the same concentration of NCs. The assessments were performed using an Ocean Insight Maya 2000 Pro high-sensitivity spectrometer with a 370 nm UV excitation source.

1.11. Texture analyzer: The mechanical properties of the NCs@PMMA microfibers mat were determined using the Brookfield AMETEK CTX instrument. The mat was subjected to compression or cutting using a knife-edge probe (TA7) with an effective width of 60 mm and a 50 kg load cell, maintaining a constant speed of 1 mm/s.

2. Synthesis of CsPbBr₃ NCs:

Firstly, the two precursor solutions were prepared in different glass vials by mixing 0.16 mmol CsBr in 2 mL DMF, and 0.16 mmol PbBr₂ in 2 mL DMF under vigorous stirring conditions. Further, 500 μ L CsBr, 500 μ L PbBr₂, 100 μ L OAc, and 50 μ L OAm solutions were mixed to make the final precursor solution, which was stirred in a vortex to get a clear solution. 1 mL of the final precursor was then injected dropwise into 10 mL toluene for the growth of NCs. The reaction was continued for 10 min and then collected in a centrifuge tube. For the isolation and purification of the NCs, 2 mL ACN, 20 μ L OAc, and 20 μ L OAm were added into the solution and then centrifuged at 6000 rpm for 15 min. The precipitate was then redispersed in toluene for further characterization.

3. Synthesis of CsPbBr₃@(OcA)₂PbBr₄ NCs:

Firstly, the three precursor solutions were prepared in different glass vials by mixing 0.16 mmol CsBr in 2 mL DMF, 0.16 mmol OcABr in 2 mL DMF, and 0.16 mmol PbBr₂ in 2 mL DMF under vigorous stirring conditions. Further, 400 μ L CsBr and 100 μ L OcABr (CsBr: OcABr= 8:2) precursor solutions were added to 500 μ L PbBr₂, 100 μ L OAc, and 50 μ L OAm to make the final precursor solution. Later, 1 mL of the final precursor was then injected dropwise into 10 mL of toluene for the growth of NCs. The reaction was continued for 10 min and then collected in a centrifuge tube. For the isolation and purification of the NCs, 2 mL ACN, 20 μ L OAc, and 20 μ L OAm were added into the solution and then centrifuged at 6000 rpm for 15 min. The precipitate was then redispersed in toluene for further characterization.

4. Tables:

4.1. Table S1: Optical properties of all the NCs:

Name of the NCs	Absorbance peak (nm)	PL peak position (nm)	Energy band gap (eV)	PLQY (%)
FC-0	520	531	2.10	50
FC-10	517	526	2.12	60
FC-20	514	521	2.14	57
FC-30	513	515	2.15	54
FCO-10	511	520	2.19	60
FCO-20	510	516	2.18	62
FCO-30	510	514	2.18	65

4.2. Table S2: Quantification of all the elements based on XPS analysis:

Element	Atomic % in FC-0	Atomic % in FC-20
C 1s	74	44.2
O 1s	14.9	3.9
Br 3p	4.7	17.6
Br 3d	4.8	14.0
Pb 4d	0	11.4
Pb 4f	1.6	6.4
Cs 3d	0	2.5

4.3. Table S3: Nonlinear optical parameters of different NCs under CW laser mode:

Sample Name	β (cm/W)	n_2 (cm ² /W)	$\chi^{(3)}$ (e.s.u.)	References
N-GO	0.14×10^{-6}	5.75×10^{-13}	3.25×10^{-7}	1
CDs	2.513×10^{-4}	1.012×10^{-8}	3.93×10^{-7}	2
CdTe	1.4×10^{-2}	2.58×10^{-7}	-	3
Red-ZnCdSeS	2.25×10^{-4}	5.89×10^{-12}	8.05×10^{-14}	4
FC-20	2.61×10^{-3}	2.52×10^{-9}	3.13×10^{-6}	This work

4.4. Table S4: Comparison of luminescent temperature sensors based on halide perovskites:

Sample Name	Range (K)	Max S_r (%-K ⁻¹)	References
CsPbBr ₃ /Cs ₄ PbBr ₆	278-328	1.01	5
CsPbBr ₃	293-353	1.2	6
CsPb(Cl/Br) ₃ : Mn ²⁺	298-335	1.4	7
CsPbBr ₃ : Eu ³⁺	93-383	2.25	8
CH ₃ NH ₃ PbBr ₃ @MOF-5	30-230	1.0	9
CsPbI ₃ : Tb ³⁺	80-480	1.78	10
CsPbBr ₃ : Dy ³⁺	80-298	2.39	11
CsPbCl ₂ Br: Eu ³⁺	80-440	3.097	12
FCO-20	303-373	3.31	This work

4.5. Table S5: Comparison of the young's modulus of different polymer based electrospun fibers:

Sample Name	Young's Modulus (MPa)	References
Polyurethane (PU) nanofibers	0.9	13
Polysulfone (PSU) nanofibers (40% RH)	1	14
Poly(ϵ -caprolactone) (PCL) fibers	3.8	15
Styrenated gelatin (StG) Microfibers	0.08	16
<i>FCO-20 NCs@PMMA fiber</i>	<i>0.82</i>	<i>This work</i>

5. Figures:

5.1. Figure S1:

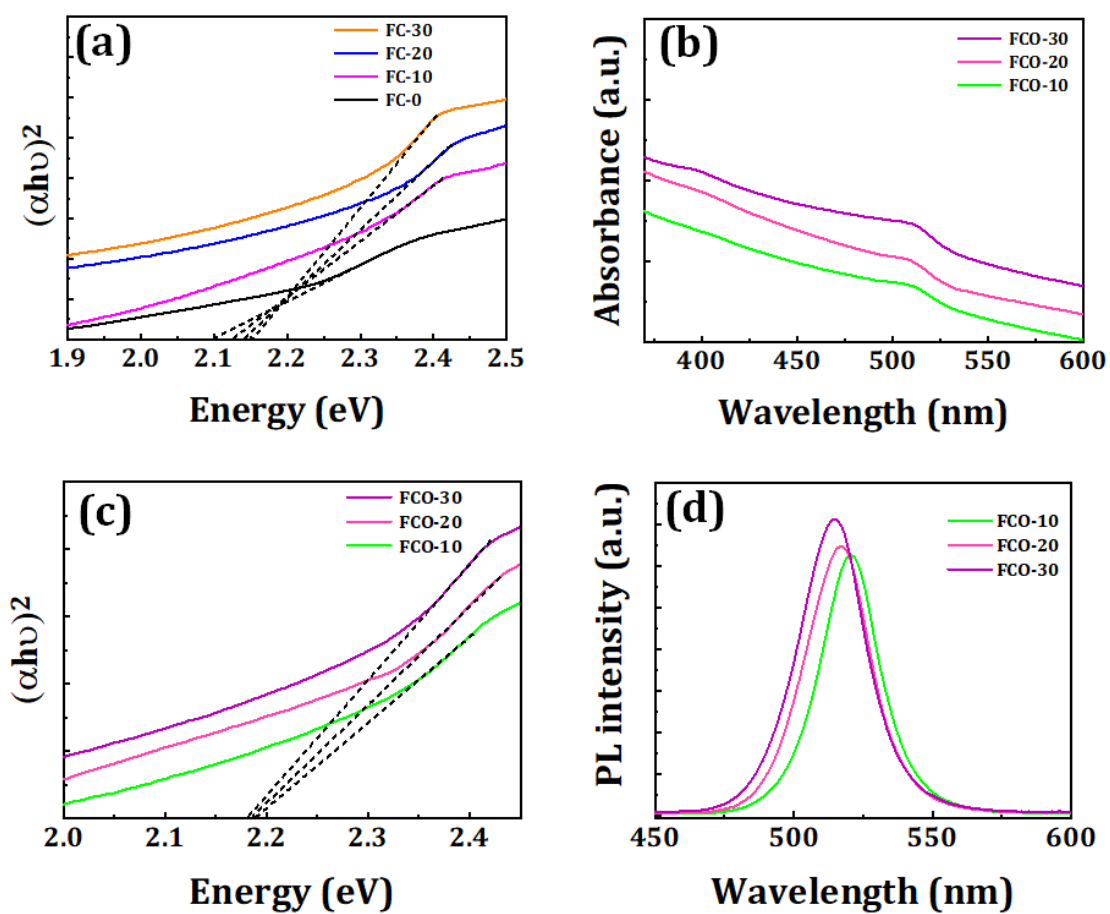


Figure S1: (a) Tauc's plot of FC-0, FC-10, FC-20, and FC-30 NCs, as shown in legend. (b) UV-Vis, (c) Tauc's plot, and (d) PL spectra of FCO-10, FCO-20, and FCO-30 NCs; as represented in legends.

5.2. Figure S2:

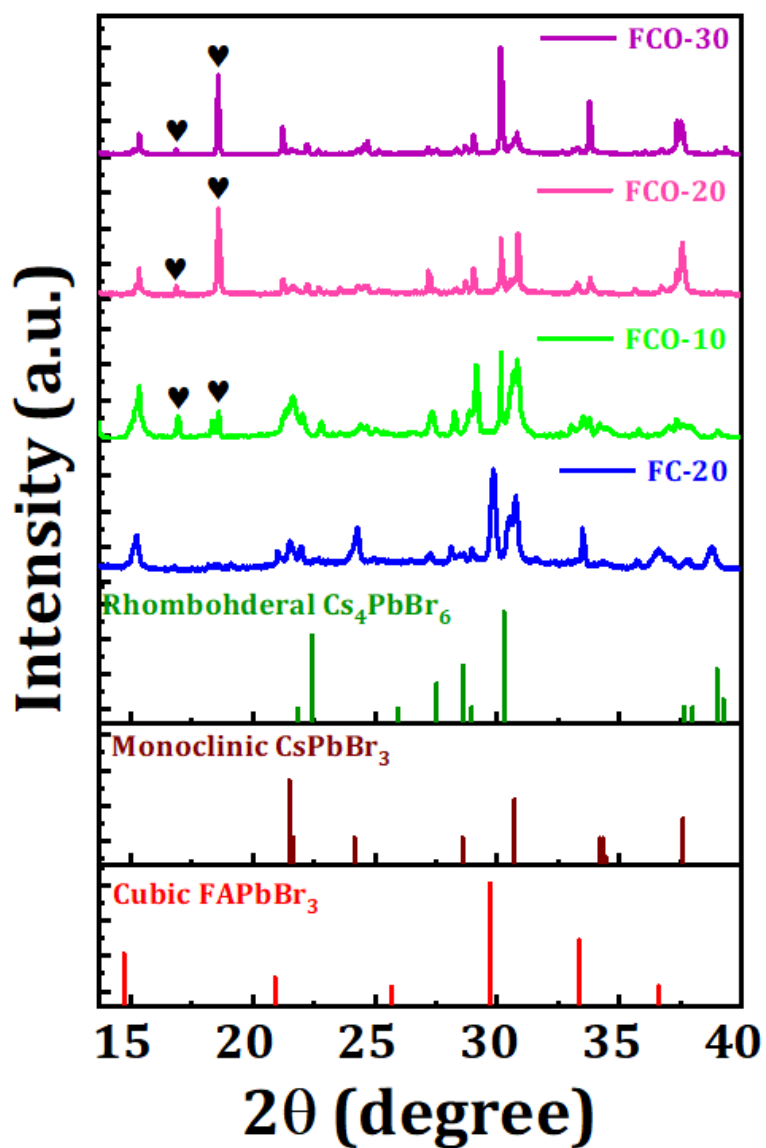


Figure S2: Stacked XRD patterns of FC-20, FCO-10, FCO-20, and FCO-30 NCs; as shown in legends. The bottom of the figure demonstrates the Cubic FAPbBr_3 , monoclinic CsPbBr_3 , and Rhombohedral Cs_4PbBr_6 crystalline phase.

5.3. Figure S3:

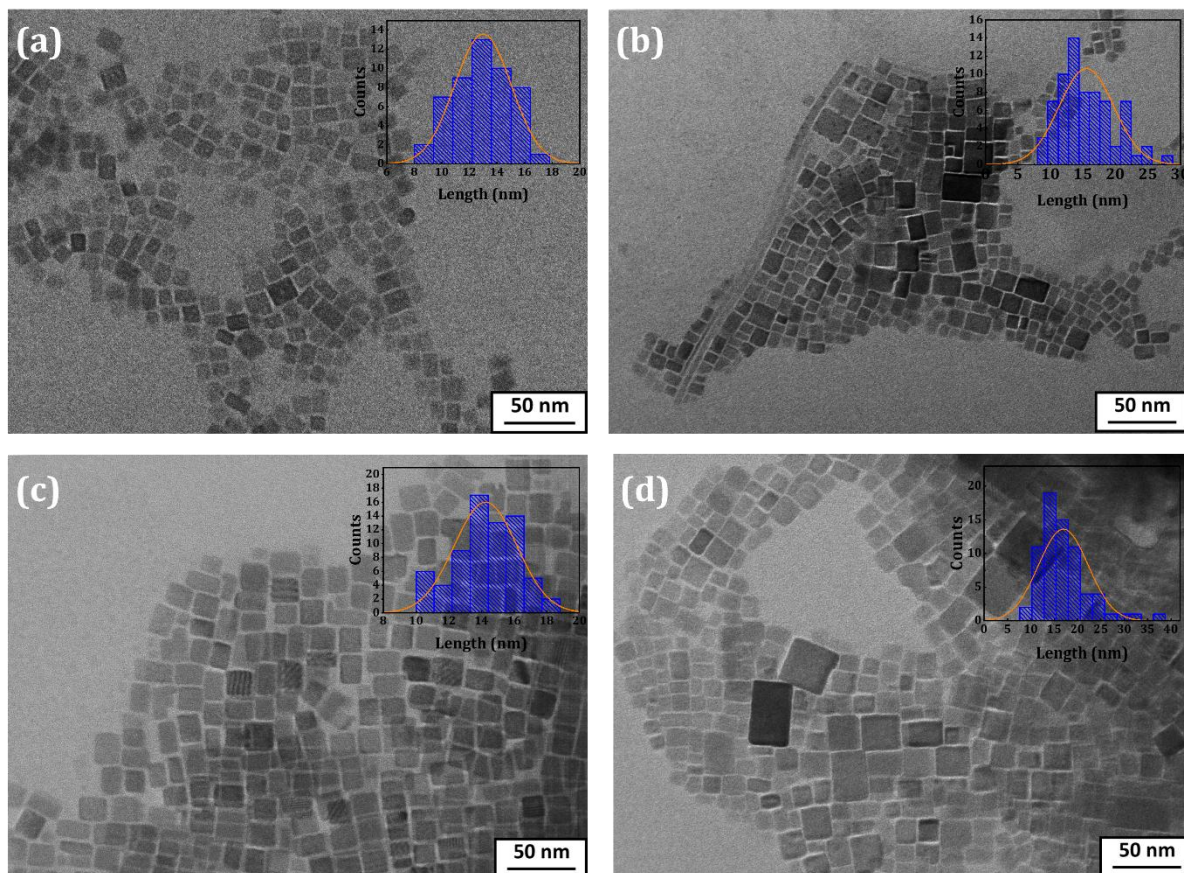


Figure S3: TEM images of (a) FC-10, (b) FC-30, (c) FCO-10, and (d) FCO-30 NCs. Inset: Size distributions of (a) FC-10, (b) FC-30, (c) FCO-10, and (d) FCO-30 NCs.

5.4. Figure S4:

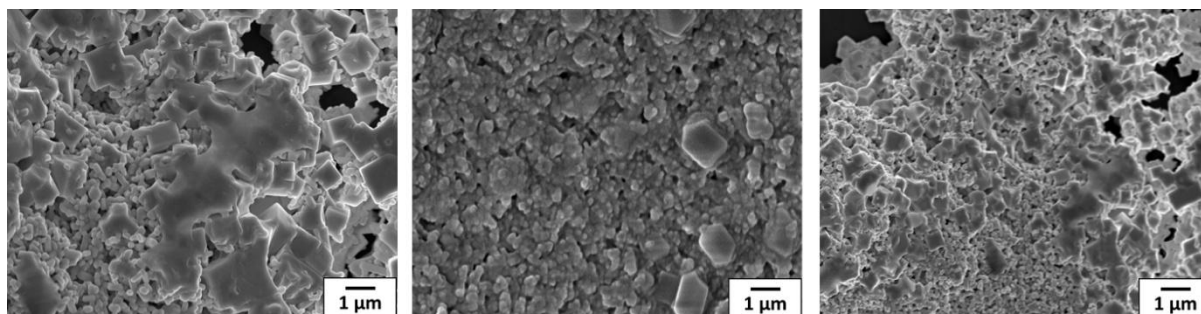


Figure S4: FESEM images of (a) FC-10, (b) FC-20, and (c) FC-30 NCs.

5.5. Figure S5:

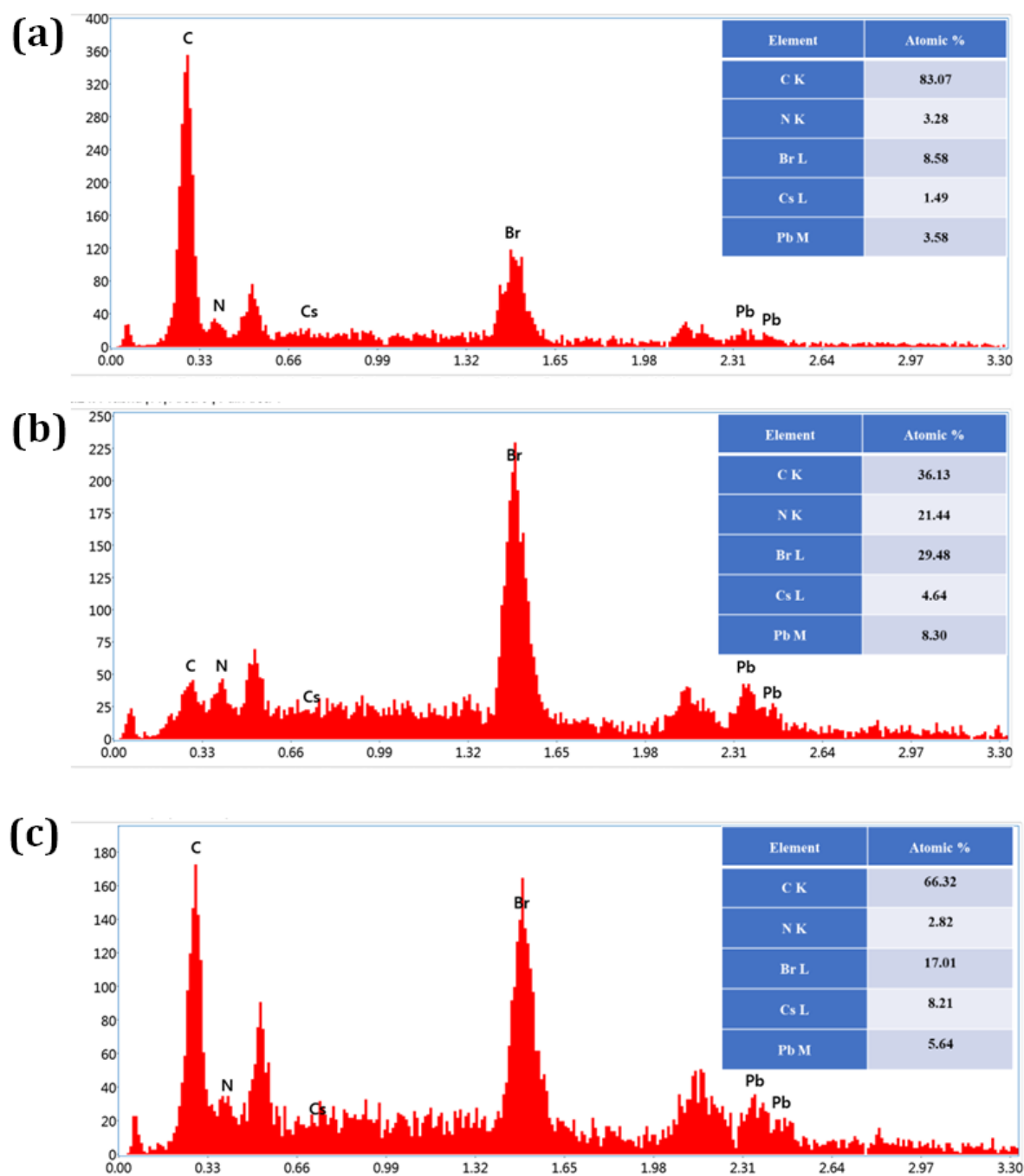


Figure S5: EDS spectrum of (a) FC-10, (b) FC-20, and (c) FC-30 NCs. Insets: atomic percentages of all the elements in tabular form.

5.6. Figure S6:

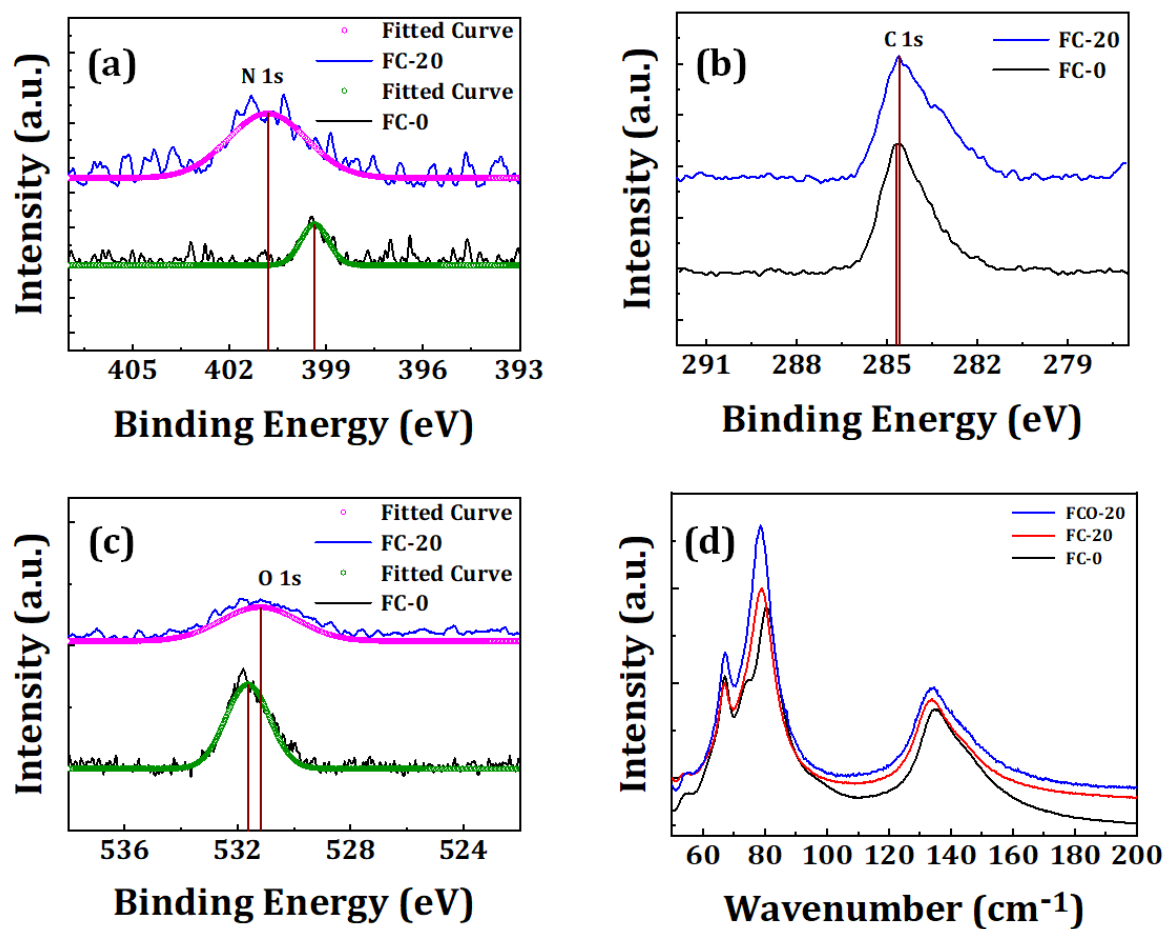


Figure S6: XPS spectra of (a) N 1s, (b) C 1s, and (c) O 1s of FC-0 and FC-20 NCs films; as shown in legends. (d) Raman spectra of FC-0, FC-20, and FCO-20 NCs films at room temperature in the range of 50-200 cm^{-1} ; as represented in legend.

5.7. Figure S7:

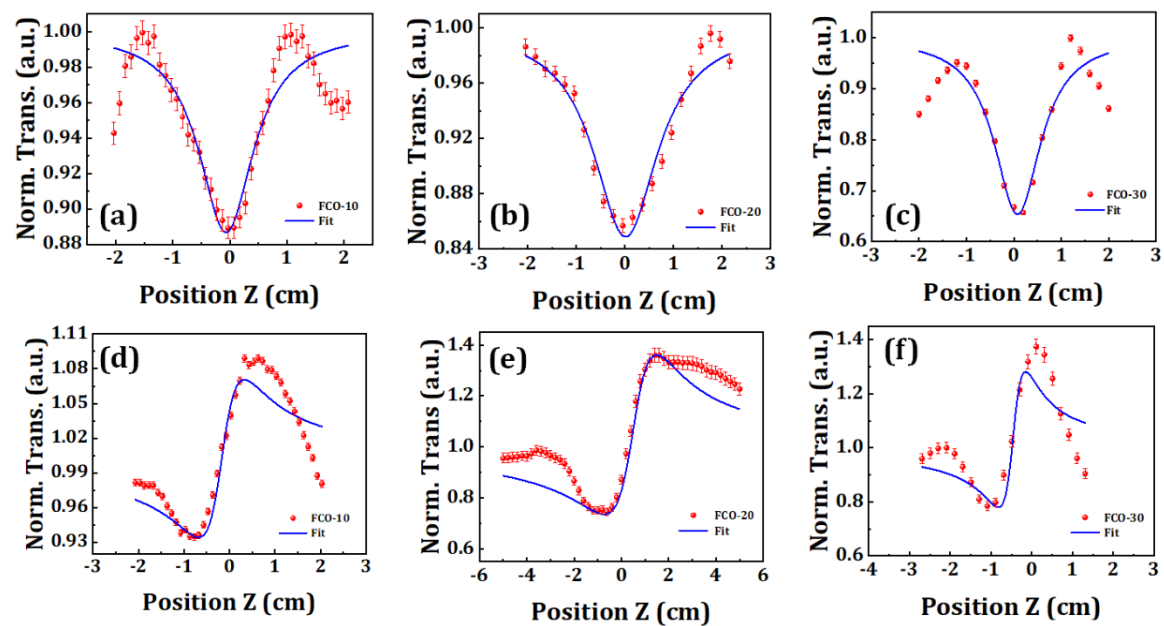


Figure S7: (a-c) Open-aperture NLO data and (d-f) Closed-aperture NLO data of FCO-10, FCO-20, and FCO-30 NCs films excited with a 532 nm CW laser, as shown in legends. **3D spheres:** Experimental Z-scan data. **Solid red line:** Theoretically fitted Z-scan data.

5.8. Figure S8:

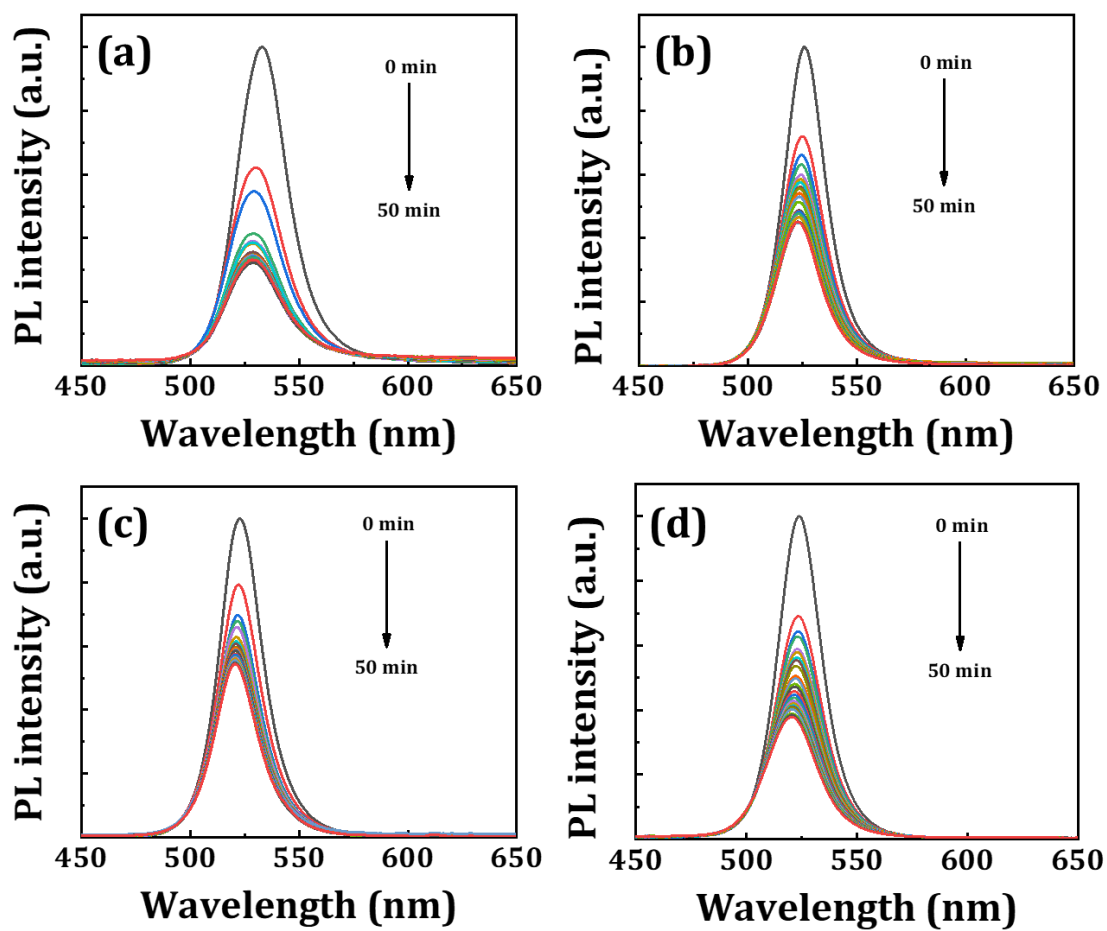


Figure S8: PL spectra of (a) FC-0, (b) FC-10, (c) FC-20, and (d) FC-30 NCs with increase in time up to 50 min, while placed on a hot plate maintained at 70 °C.

5.9. Figure S9:

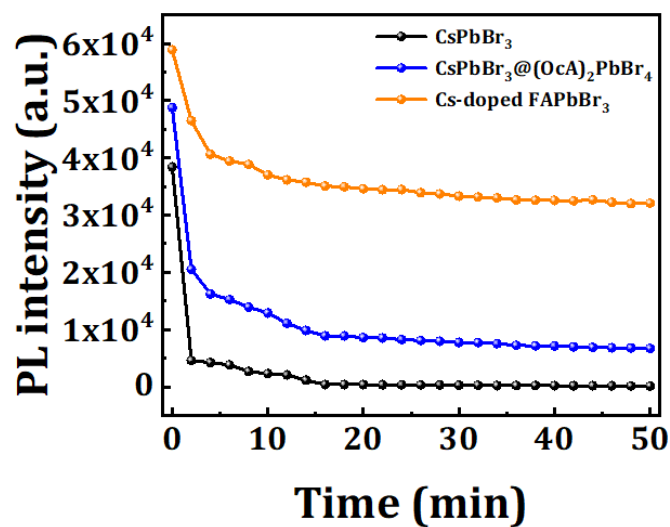


Figure S9: Relative change in PL intensities concerning the time of all the NCs' films while placed on a hot plate maintained at 70 °C, as shown in legends.

5.10. Figure S10:

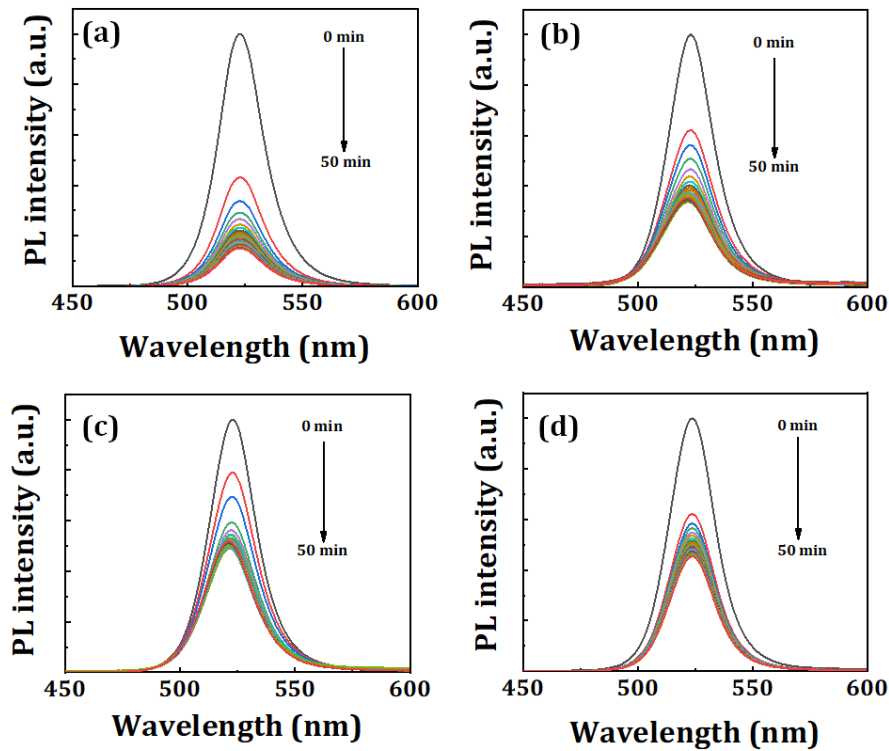


Figure S10: PL spectra of (a) FC-20, (b) FCO-10, (c) FCO-20, and (d) FCO-30 NCs films with an increase in time for 50 min, while placed on a hot plate maintained at 70 °C.

5.11. Figure S11:

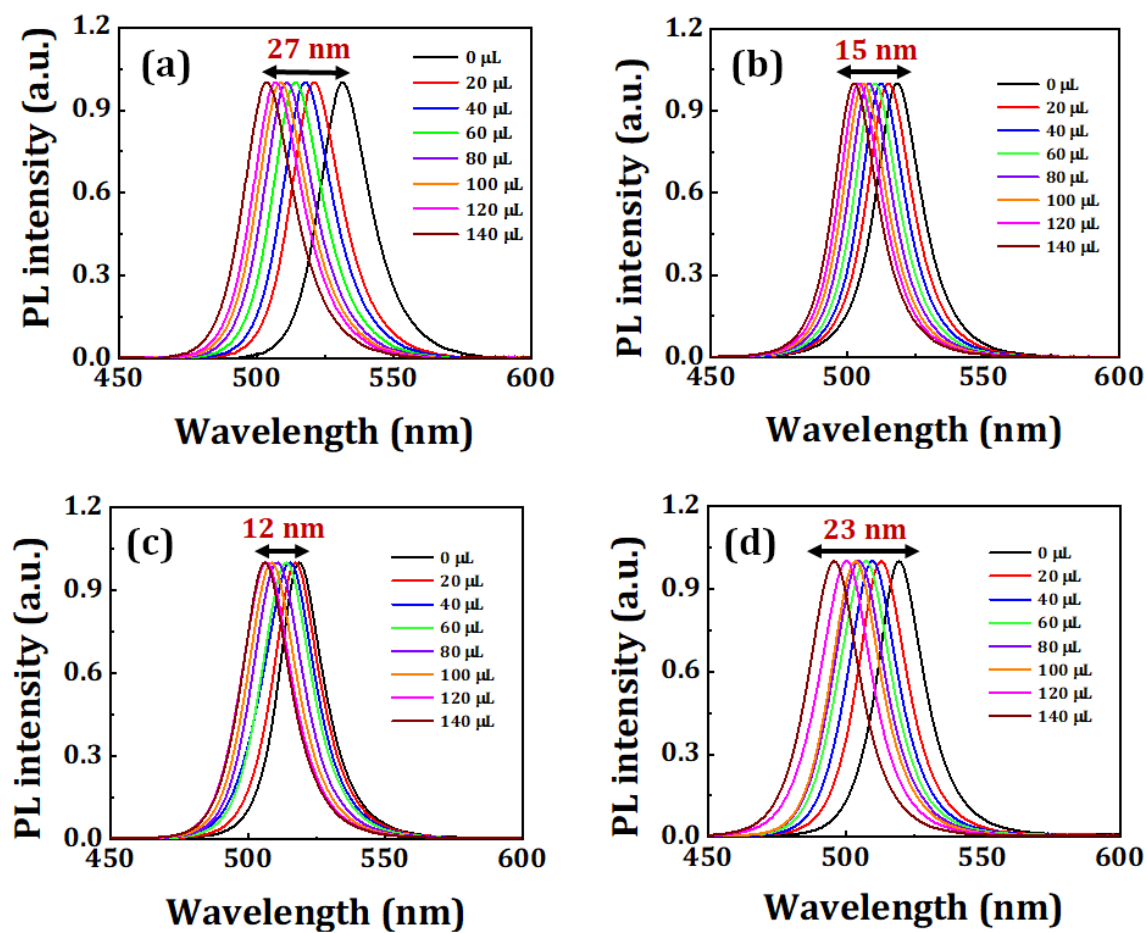


Figure S11: Normalized PL spectra of (a) FC-0, (b) FC-10, (c) FC-20, and (d) FC-30 NCs solutions after the addition of TBA-Cl precursor solution.

5.12. Figure S12:

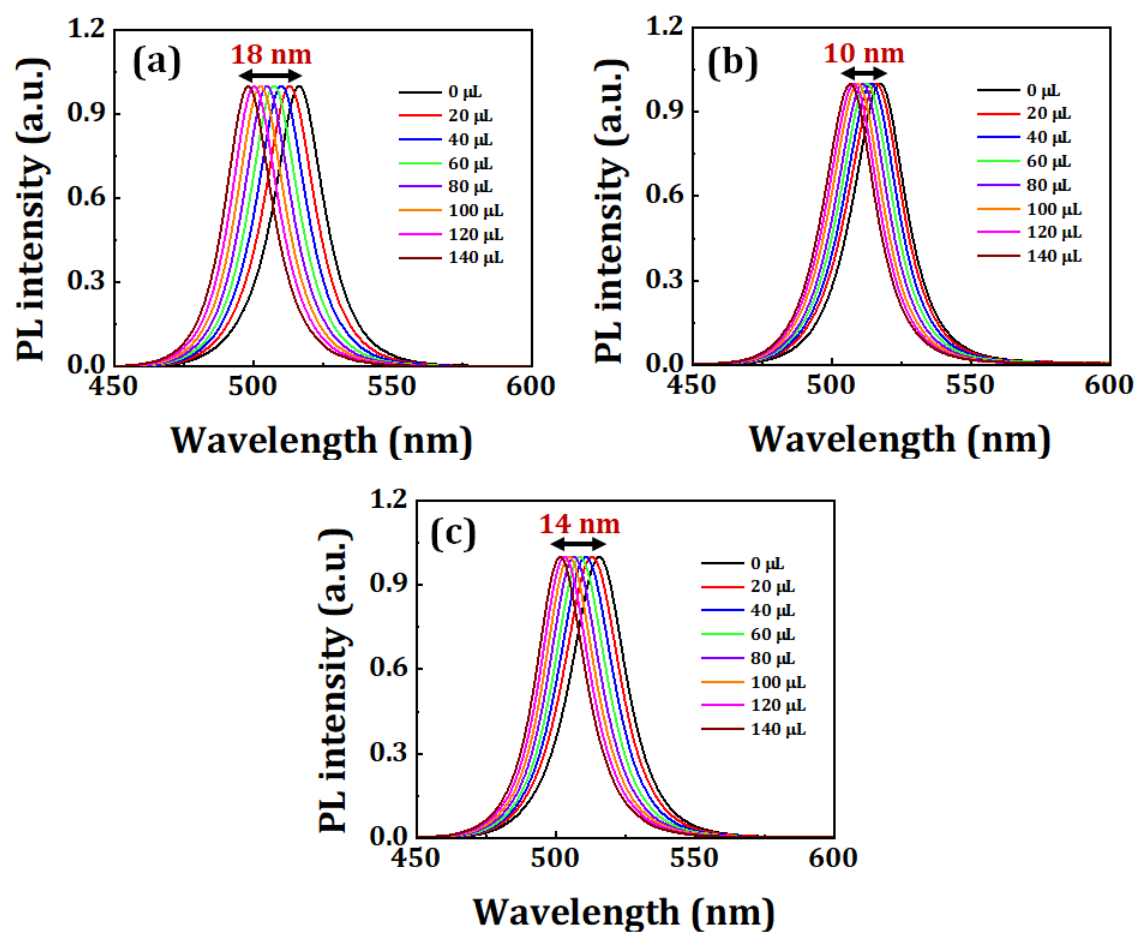


Figure S12: Normalized PL spectra of (a) FCO-10, (b) FCO-20, and (c) FCO-30 NCs solutions after the addition of TBA-Cl solution.

5.13. Figure S13:

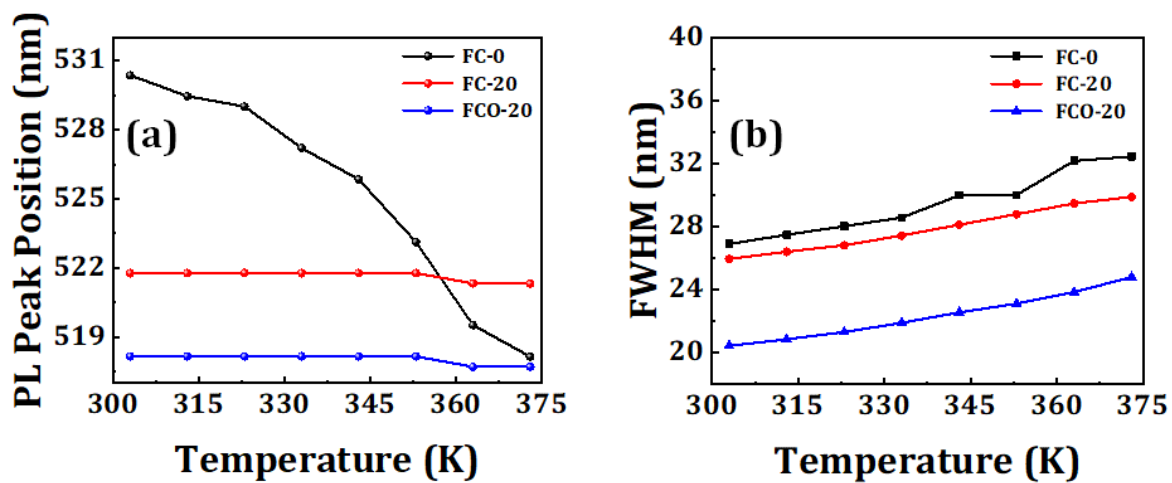


Figure S13: (a) Relative change in PL peak position, and (b) Change in FWHM with increase in temperature from 303 to 373 K of all the NCs films, as shown in legends.

5.14. Figure S14:

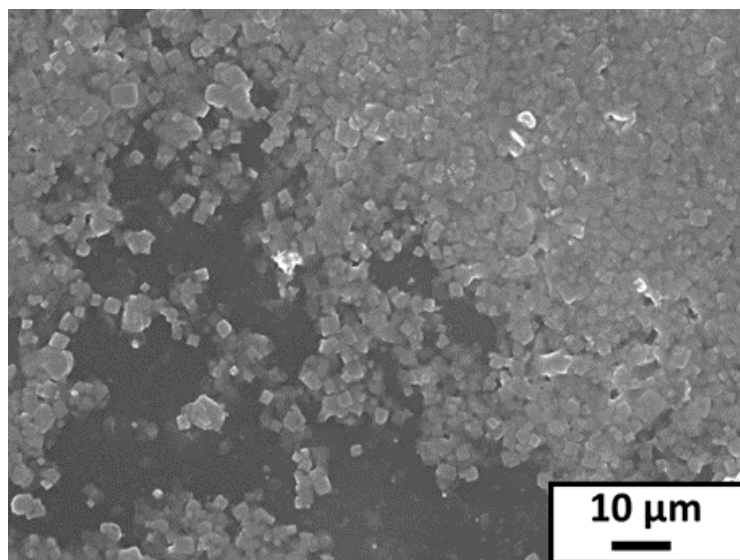


Figure S14: FESEM image of FCO-20 NCs film.

5.15. Figure S15:

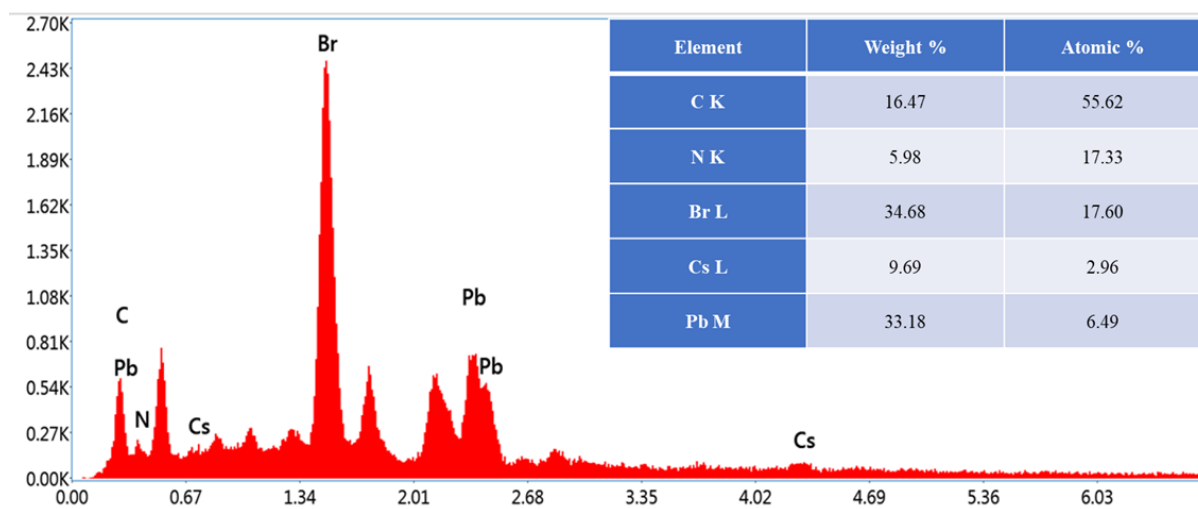


Figure S15: EDS spectrum of FCO-20@PMMA Fiber film showing all the elements present on the surface. Inset: EDS data obtained from FESEM image showing both the weight and atomic percentage of different elements.

5.16. Figure S16:

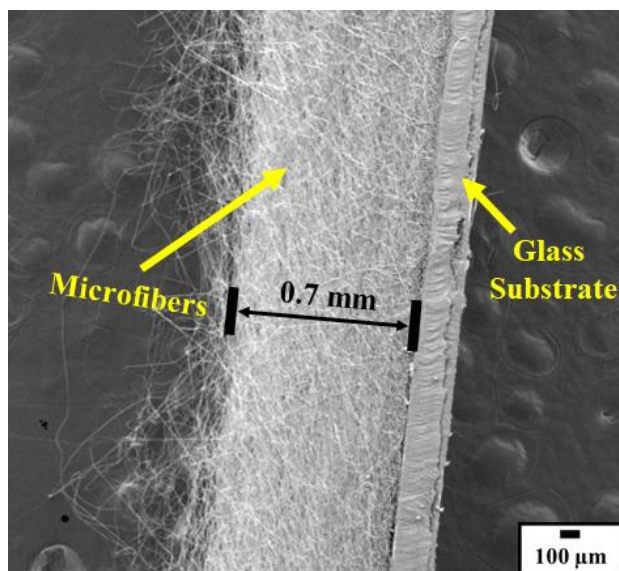


Figure S16: FESEM image of the cross-sectional view of FCO-20 NCs@Fiber film on the glass substrate.

5.17. Figure S17:

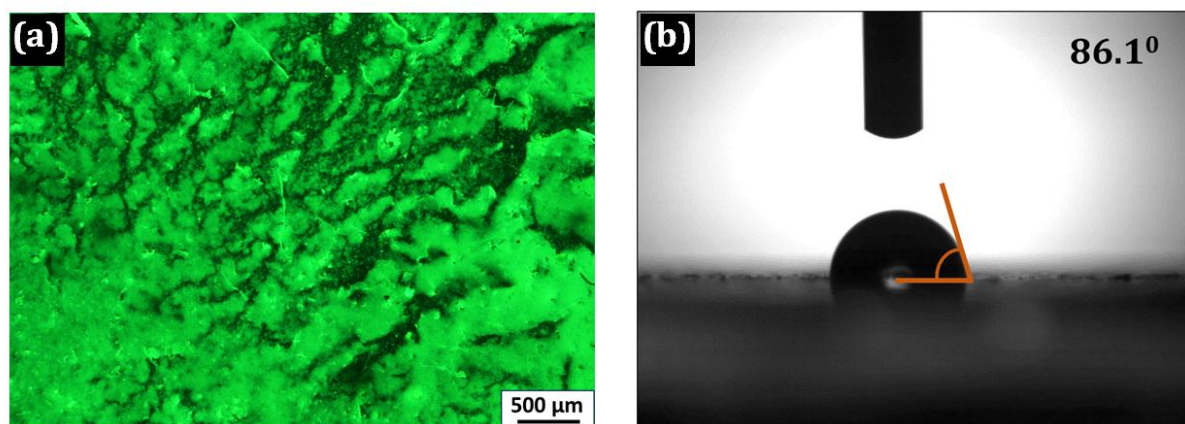


Figure S17: (a) Fluorescence microscopic image and (b) contact angle measurement of FCO-20 NCs film.

5.18. Figure S18:

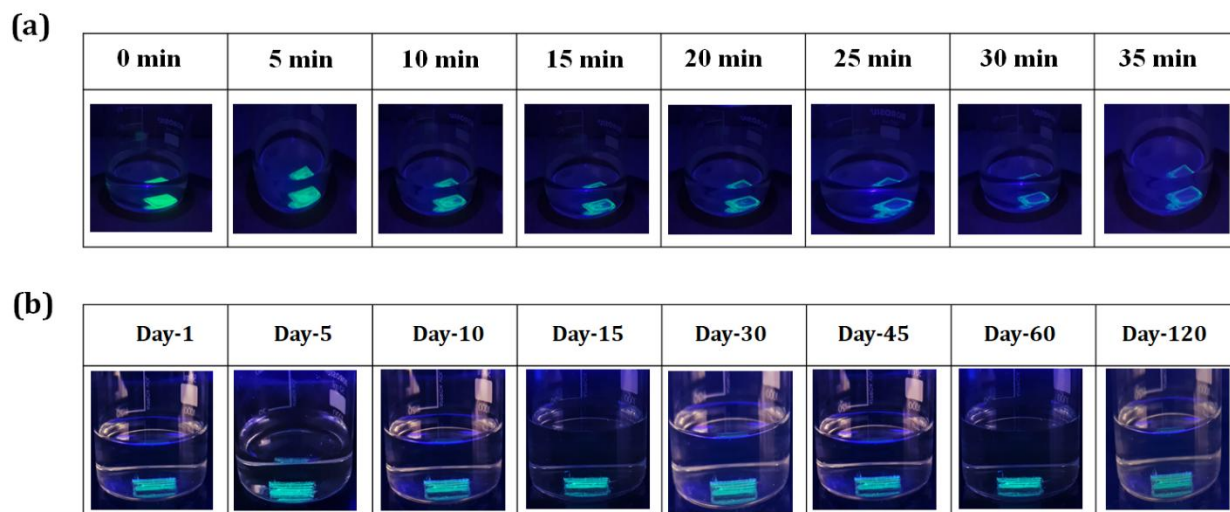


Figure S18: Water stability test of (a) FCO-20 NCs and (b) FCO-20@PMMA microfibers by dipping the films in water.

5.19. Figure S19:

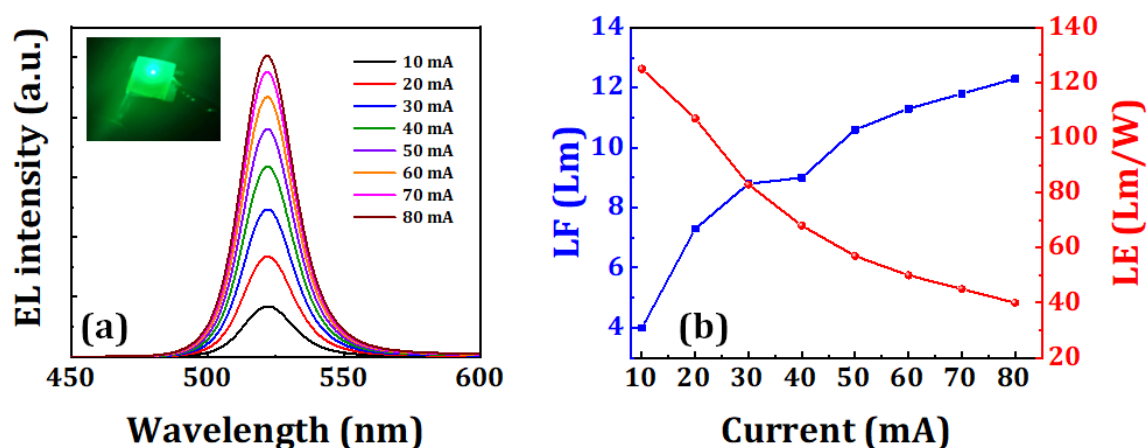


Figure S19: (a) EL spectra of FCO-20 NCs based G-LED with increase in current from 10-mA to 80-mA. Inset: photographic image of the G-LED under biasing condition. (b) Relationship between Luminous flux and LE of as fabricated G-LED.

References:

1. K. Kumara, T. C. S. Shetty, S. R. Maidur, P. S. Patil and S. M. Dharmaprakash, *Optik*, 2019, **178**, 384-393.
2. S. Pandiyan, L. Arumugam, S. P. Srengan, R. Pitchan, P. Sevugan, K. Kannan, G. Pitchan, T. A. Hegde and V. Gandhirajan, *ACS Omega*, 2020, **5**, 30363-30372.
3. M. H. Majles Ara, Z. Moslemi, H. Naderi, A. Mihandoost, A. Daneshfar and R. Sahraei, *Appl. Phys.B*, 2015, **118**, 567-572.
4. Z. Moslemi, E. Soheyli, M. H. M. Ara and R. Sahraei, *J. Phys. Chem. Solids*, 2018, **120**, 64-70.
5. Z. Lu, Y. Li, Y. Xue, W. Zhou, S. Bayer, I. D. Williams, A. L. Rogach and S. Nagl, *ACS Appl. Nano Mater.*, 2022, **5**, 5025-5034.
6. Z. Lu, Y. Li, W. Qiu, A. L. Rogach and S. Nagl, *ACS Appl. Mater. Interfaces*, 2020, **12**, 19805-19812.
7. D. Chen, G. Fang, X. Chen, L. Lei, J. Zhong, Q. Mao, S. Zhou and J. Li, *J. Mater. Chem. C*, 2018, **6**, 8990-8998.
8. X. Li, Y. Yu, J. Hong, Z. Feng, X. Guan, D. Chen and Z. Zheng, *J. Lumin.*, 2020, **219**, 116897.
9. D. Zhang, Y. Xu, Q. Liu and Z. Xia, *Inorg. Chem.*, 2018, **57**, 4613-4619.
10. Y. Zhang, J. Liu, H. Zhang, Q. He, X. Liang and W. Xiang, *J. Eur. Ceram. Soc.*, 2020, **40**, 6023-6030.
11. G. Yao, S. Li, D. Valiev, Q. Chen, Y. Hu, L. Jia, S. Stepanov, Y. Zhou, C. Li and Z. Su, *Opt. Mater.*, 2021, **122**, 111711.
12. Y. Yu, G. Shao, L. Ding, H. Zhang, X. Liang, J. Liu and W. Xiang, *J. Rare Earth.*, 2021, **39**, 1497-1505.
13. J. Zhou, Q. Cai, X. Liu, Y. Ding and F. Xu, *Nanoscale Res. Lett.*, 2018, **13**, 1-5.
14. L. Huang, N. N. Bui, S. S. Manickam and J. R. McCutcheon, *J. Polym. Sci. Part B: Polym. Phys.*, 2011, **49**, 1734-1744.
15. F. Croisier, A. S. Duwez, C. Jérôme, A. F. Léonard, K. O. Van Der Werf, P. J. Dijkstra and M. L. Bennink, *Acta Biomater.*, 2012, **8**, 218-224.
16. D. Huang, Y. Nakamura, A. Ogata and S. Kidoaki, *Polym. J.*, 2020, **52**, 333-344.